UNIVERSITY OF BIRMINGHAM
University of Birmingham Research at Birmingham

Hollow spheres as nanocomposite fillers for aerospace and automotive composite materials applications

Lapčík, Lubomír; Ruszala, Matthew J.a.; Vašina, Martin; Lapčíková, Barbora; Vlček, Jakub; Rowson, Neil A.; Grover, Liam M.; Greenwood, Richard W.

DOI:
10.1016/j.compositesb.2016.09.031

License:
Creative Commons: Attribution-NonCommercial-NoDerivs (CC BY-NC-ND)

Document Version
Peer reviewed version

Citation for published version (Harvard):
Lapčík, L, Ruszala, MJA, Vašina, M, Lapčíková, B, Vlček, J, Rowson, NA, Grover, LM & Greenwood, RW 2016, 'Hollow spheres as nanocomposite fillers for aerospace and automotive composite materials applications', *Composites Part B: Engineering*, vol. 106, pp. 74-80. https://doi.org/10.1016/j.compositesb.2016.09.031

Link to publication on Research at Birmingham portal

Publisher Rights Statement:
Checked 11/11/2016

General rights
Unless a licence is specified above, all rights (including copyright and moral rights) in this document are retained by the authors and/or the copyright holders. The express permission of the copyright holder must be obtained for any use of this material other than for purposes permitted by law.

•Users may freely distribute the URL that is used to identify this publication.
•Users may download and/or print one copy of the publication from the University of Birmingham research portal for the purpose of private study or non-commercial research.
•User may use extracts from the document in line with the concept of 'fair dealing' under the Copyright, Designs and Patents Act 1988 (?)
•Users may not further distribute the material nor use it for the purposes of commercial gain.

Where a licence is displayed above, please note the terms and conditions of the licence govern your use of this document.

When citing, please reference the published version.

Take down policy
While the University of Birmingham exercises care and attention in making items available there are rare occasions when an item has been uploaded in error or has been deemed to be commercially or otherwise sensitive.

If you believe that this is the case for this document, please contact UBIRA@lists.bham.ac.uk providing details and we will remove access to the work immediately and investigate.

Download date: 04. May. 2023

Accepted Manuscript

Hollow spheres as nanocomposite fillers for aerospace and automotive composite materials applications

Lubomír Lapčík, Matthew J.A. Ruszala, Martin Vašina, Barbora Lapčíková, Jakub Vlček, Neil A. Rowson, Liam M. Grover, Richard W. Greenwood

PII: S1359-8368(16)31510-4

DOI: 10.1016/j.compositesb.2016.09.031

Reference: JCOMB 4523

To appear in: *Composites Part B*

Received Date: 4 August 2016

Accepted Date: 12 September 2016

Please cite this article as: Lapčík L, Ruszala MJA, Vašina M, Lapčíková B, Vlček J, Rowson NA, Grover LM, Greenwood RW, Hollow spheres as nanocomposite fillers for aerospace and automotive composite materials applications, *Composites Part B* (2016), doi: 10.1016/j.compositesb.2016.09.031.

This is a PDF file of an unedited manuscript that has been accepted for publication. As a service to our customers we are providing this early version of the manuscript. The manuscript will undergo copyediting, typesetting, and review of the resulting proof before it is published in its final form. Please note that during the production process errors may be discovered which could affect the content, and all legal disclaimers that apply to the journal pertain.

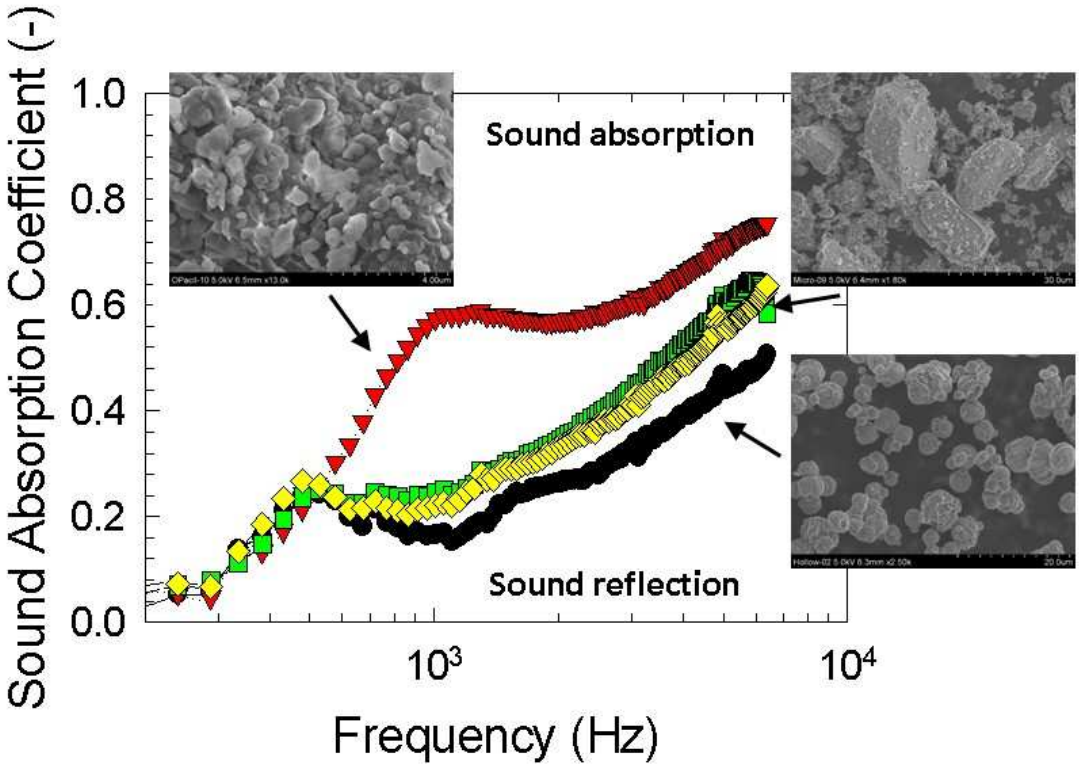

ACCEPTED MANUSCRIPT

ACCEPTED MANUSCRIPT

Hollow spheres as nanocomposite fillers for aerospace and automotive composite materials applications

Lubomír Lapčík[*1,2], Matthew J.A. Ruszala[3], Martin Vašina[4,5], Barbora Lapčíková[1,2], Jakub Vlček[1], Neil A. Rowson[3], Liam M. Grover[3], Richard W. Greenwood[3]

[1]Regional Centre of Advanced Technologies and Materials, Department of Physical Chemistry, Faculty of Science, Palacky University, 17. Listopadu 12, 771 46 Olomouc, Czech Republic

[2]Tomas Bata University in Zlin, Faculty of Technology, Inst. Foodstuff Technology, Nam. T.G. Masaryka 275, 760 01 Zlin, Czech Republic

[3]School of Chemical Engineering, University of Birmingham, Edgbaston, Birmingham, B15 2TT, UK

[4]Tomas Bata University in Zlin, Faculty of Technology, Inst. Physics Materials Engineering, Nam. T.G. Masaryka 275, 760 01 Zlin, Czech Republic

[5]VŠB-Technical University of Ostrava, Department of Hydromechanics and Hydraulic Equipment, Faculty of Mechanical Engineering, 17. Listopadu 15/2172, 708 33 Ostrava-Poruba, Czech Republic

[*]Corresponding author: L. Lapčík, Regional Centre of Advanced Technologies and Materials, Department of Physical Chemistry, Faculty of Science, Palacky University, 17. Listopadu 12, 771 46 Olomouc, Czech Republic. Tel.: +420 732506770.

Email: lapcikl@seznam.cz (L. Lapčík).

ACCEPTED MANUSCRIPT

ABSTRACT

There were studied four types of powder filler materials for polyolefin composite parts production for automotive and aerospace industry. There was confirmed, that the particle shape has a strong effect on the acoustic and mechanical properties of the powder bed as influenced by the varying packing density. The calcium carbonate spherical hollow particles exhibited the best aerodynamic performance when aerated and were completely fluidized. Simultaneously they were exhibiting the easy flowing behaviour as reflected in the observed flowability of 4.71. In contrary to this, the flat lamellar geometry of the precipitated calcium carbonate resulted in the worst fluidization behaviour, as the aeration energy was 2.5× higher in comparison to the spherical particles. Remaining samples under study, i.e. flash calcined kaolin and dolomite powder, exhibited cohesive rheological behaviour as reflected in the observed flowability. There was found a clear correlation between powder rheological and electrostatic charge data with the observed acoustic performance as reflected in the frequency dependence of the normal incident sound damping coefficient. This was demonstrated by a relatively high increase in the damping efficiency with increasing porosity of the powder bed as reflected in the decreasing packing density. However the best fit was found between the absolute value of the electrostatic charge values and the sound damping properties.

Keywords: Hollow sphere particles; Powder rheology; Sound damping; Powder processing; Elastic coefficient; Electrostatic charge.

1. Introduction

At present there is an increased demand for the application of synthetic polymers in the automotive and aeronautic industries. It is mainly targeted for utilisation of poly(ethylene), poly(propylene), polycarbonate and polyamide components of the interior, exterior or other

ACCEPTED MANUSCRIPT

functional parts of vehicles [1,2]. Minerals first served as additives in polymer systems as a cost reducing technology [3] and due to the technological improvements in minerals processing and polymer chemistry, these materials are now used as functional additives [4] bringing specific mechanical and functional properties to the final composite products [5,6]. For example, hollow particle filled composites, called syntactic foams, are used in applications requiring high damage tolerance and low density, e.g. in aerospace and marine engineering structural applications. It was found that the presence of stiff hollow inclusions can enhance the composite elastic modulus in comparison to neat resin. Moreover, with the latter elastic modulus enhancement, an increase in energy absorption under compressive load was found due to the hollow fillers progressively crushing [6].

The recent review article by Wang et al. [7] described the present state of the art chemical synthesis routes and strategies for the synthesis of hollow micro/nano structured materials. The synthetic strategies were grouped into three major categories; hard templating, soft templating, and self-templating synthesis. Hollow spheres have a wide range of applications due to their regular uniform shape, meaning that they have the same properties, regardless of their orientation. Nano/micro scale hollow spheres have been produced through a variety of different methods [8-15] and have the benefit of being a colloidal particle that can flow, and remain untangled with other particles when put into a complex formulation [16]. Hollow latex spheres have been made commercially since the 1980's [17,18], with the primary production method being osmotic swelling [19]. Hollow latex spheres however have the disadvantage of being easily squashed or ruptured, so sturdier mineral structures are often preferred. This can be achieved by armour plating hollow latex spheres [20,21], or by creating hollow spheres directly from mineral structures, which has the benefit of fewer production steps.

Creating hollow spheres made of calcium carbonate has proved to be a success, with [22], and [23] making them using a carbon dioxide bubbles as a template, whilst [24,25] used an

ACCEPTED MANUSCRIPT

emulsification process. Consequently, hollow $CaCO_3$ spheres have proved to be a success, and the understanding of their properties, and their possible applications continue to increase.

Another route for the production of the perfectly formed dense agglomerates and the formation of deformed or hollow agglomerates is affected by particle consolidation during spray drying evaporation, particle rearrangement during the consolidation period and by the inter-particle potential. In general, the consolidation can proceed in the thermodynamic state, where the inter-particle potential is either repulsive or attractive. In the dispersed slurry, the long-range inter-particle potential allows the particles to repel one another. When the particles are repulsive, the meniscus that separates the two fluids exerts a capillary pressure on the particles at the surface, forcing them together as a dense agglomerates. In the case of the mechanism, where particles were not allowed to rearrange after a short period of evaporation, the agglomerate becomes hollow and deformed. Whereas in the case of the attractive particle network, if the capillary pressure exceeds the yield stress, the spherical agglomerates with uniform density are formed [26].

As a composite system matrix, polyolefin polymers are widely used, such as poly(ethylene) or poly(propylene), with different grades, types and qualities [3]. There was found to be an increase in tested polyolefin melts viscosity, a decrease of the elasticity with increasing filler loading and the presence of yield values in the flow curves depending on the filler particles volume loading and particles size [27]. When comparing the acoustic properties of the composite materials, the process of the interaction of the mechanical acoustic wave and the material structure is based on the assumption that an incoming wave is reflected at the boundary between two acoustically different materials due to the differences in the acoustic impedance of the involved materials [28-31].

ACCEPTED MANUSCRIPT

This paper is focused on the application of powder rheology, acoustic performance testing and electrostatic charge measurements on the evaluation of hollow spheres and lamellar mineral powder materials as prospective fillers for polyolefin composite materials applications.

2. Theoretical background

Sound is an acoustic wave with frequencies ranging from 10 Hz to 16 kHz, with sonic waves spreading in all directions from the source. On the basis of different points of view on the problem of noise attenuation it is possible to distinguish the following methods of sound and vibration damping [32]:

– Reduction method – attenuation at the noise source, e.g. during the machinery construction stage.

– Sound isolation method – covering the sound source by material with high airborne sound insulation characteristics.

– Sound absorption method – endeavour to minimise sound reflections e.g. to absorb the maximum of the incident acoustic energy.

In the matrix of the sound/vibration attenuating material, dissipation of the sonic wave to mechanical energy and heat takes place. This proceeds by the combination of the following processes:

– By friction of the vibrating air particles on the walls during their penetration into the pores of the sound absorbing material. This lowers the kinetic energy of the incident sound field. Effectiveness of this process increases with growing porosity of the absorption material.

– By decreasing the potential energy of the sonic wave penetrating into the material. This lowers the acoustic pressure due to the heat exchange between air and the skeleton of the absorbing material during periodic pressure changes.

ACCEPTED MANUSCRIPT

– By non-elastic deformation of the absorbing material body. At the specifically aimed construction of the vibration or noise–isolation material it is therefore possible to utilise all of the above mentioned processes for their synergistic effect in obtaining maximum effectiveness of attenuation. This is possible by modelling the geometry of the damping material body as well as by proper selection of the main material matrix and adhesive system.

2.1. Sound absorption measurements

Sound absorption properties express a material's ability to absorb incident acoustic energy and is described by the sound absorption coefficient (α) which is defined by the ratio of dissipated power in a tested material and incident power. Sound absorption of a given material depends on many factors, including; excitation frequency, thickness, structure, temperature, density and humidity [28,32]. The effect of the excitation frequency on the sound absorption coefficient is expressed by the noise reduction coefficient (NRC), which is defined as the arithmetic mean of the sound absorption coefficients of a given material at the excitation frequencies of 250, 500, 1000 and 2000 Hz [33]. On the basis of the primary absorption peak frequency (f_{p1}), it is possible to determine the speed of sound (c) of an elastic wave through a powder bed and the longitudinal elastic coefficient (K) of the power bed as follows, where h is the height of a given powder bed and ρ_b is the bulk density of the powder bed. [34]:

$$\boldsymbol{c = 4\, f_{p1}\, h} \tag{1}$$

$$\boldsymbol{K = c^2 \rho_b = 16 f_{p1}^2\, h^2\, \rho_b} \tag{2}$$

3. Materials

ACCEPTED MANUSCRIPT

The materials studied were commercially available mineral filler powders and are described in Table 1. Four samples were analysed; formulated calcium carbonate spheres (process route developed at The University of Birmingham, UK), flash calcined kaolin, dolomite and calcined kaolin. Samples 1 was the hollow calcium carbonate spheres, sample 2 was flash calcined kaolin based filler (Imerys, UK), sample 3 was dolomite powder (CaO (30.3 wt.%), MgO (21.6 wt.%), Fe_2O_3 (0.08 wt.%)) (Omya, Switzerland) and sample 4 was a calcined kaolin based filler (Imerys, UK). Sample moisture content ranged from 0.1 to 0.9 wt.%.

4. Methods

4.1. Scanning Electron Microscopy

Scanning electron microscopy (SEM) was used to determine the shape and size of the studied mineral composite filler particles. SEM images were captured using a Hitachi 6600 FEG microscope (Japan) operating in the secondary electron mode using an accelerating voltage of 1 kV.

4.2. Thermal Analysis

Thermogravimetry (TG) and differential thermal analysis (DTA) experiments were performed on simultaneous DTA-TG apparatus (Shimadzu DTG 60, Japan) to determine the moisture content of the samples, and to determine whether there was any organic material present. Throughout the experiment, the sample temperature and weight-heat flow changes were continuously monitored. The measurements were performed at a heat flow rate of 10 °C/min in a static air atmosphere at the temperature range of 30 °C to 300 °C.

4.3. Powder rheology

ACCEPTED MANUSCRIPT

Powder rheology measurements were conducted on a FT4 Powder rheometer (Freeman Technology, UK). All experiments were performed under the ambient laboratory conditions of 23 ℃ and relative humidity of 43 %.

4.4. Acoustic performance testing

The frequency dependencies of the sound absorption coefficients of the investigated powders were experimentally determined by the transfer function method ISO 10534-2 [31,35,36]. The frequency dependencies were experimentally measured using a two-microphone impedance tube BK 4206 in combination with a three-channel signal Pulse Multianalyzer BK 3560-B-030 and power amplifier BK 2706 (all from Brüel & Kjær, Denmark) in the frequency range of 150-6400 Hz. This equipment was subsequently used in order to determine the noise reduction coefficient, the speed of sound through the loose powder materials and the longitudinal elastic coefficient of the investigated unconsolidated materials. The normal incidence sound wave absorption of the investigated loose powder samples of defined layer thickness (ranging from 5 to 100 mm) was also determined. The measurements were performed under ambient laboratory conditions of 62 % relative humidity and at constant temperature of 25 °C.

4.5. Electrostatic charge measurements

Electrostatic charge measurements were conducted on a NK-1001A Coulomb meter (Kasuca Denki, Japan). Samples were placed in a Faraday cage and the charge (nC) was measured for 1 g samples [37]. Each measurement was repeated 8×, and all measurements were performed at 25 ℃ ambient laboratory temperature and 45 % relative humidity.

ACCEPTED MANUSCRIPT

5. Results and discussion

Sound absorption properties of the tested powders are affected by their porosity, shape of pores, angle of inclination of incident acoustic waves on the material surface, friction of acoustic waves during transmission through the porous matrix [32], material mechanical stiffness and conditions of applied acoustic field, including; sound excitation frequency, ambient air relative humidity and ambient temperature. The shape and size of the tested powder materials observed using SEM are shown in Fig. 1. Sample 1 was found to have a regular spherical shape with a narrow 4 μm diameter, whilst sample 2 had a plate agglomerate structure of 3-6 μm particle dimensions, contrary to the agglomerate structure of sample 2, samples 3 and 4 exhibited lamellar plate like structures of 20 to 30 μm dimensions with a relatively large fraction of the residual 3 to 4 μm size particles.

Results of the normal incidence sound absorption measurements are shown in Figs. 2 and 3 and are summarised in Table 2. From this data it is evident that sound absorption properties increase with increasing material thickness, in this case with height of the loose powder bed. Fig. 2 demonstrates the measured data for hollow spheres (sample 1). The obtained frequency dependencies of the normal incidence sound absorption coefficient are characterised by the primary absorption peak at a characteristic frequency f_{p1}. It is visible that the primary absorption peak frequency was shifted toward decreasing frequency with increasing loose powder bed height (Fig. 2), i.e. from 1584 Hz for the bed height of 5 mm to 304 Hz for 100 mm powder bed height. Similar dependencies of the f_{p1} on the powder bed height were also observed for the other materials tested (Table 2). As was described in the theoretical section, the primary absorption peak frequency is directly proportional to the longitudinal elastic coefficient of the powder bed and to the velocity of the sound propagation through the powder bed. There was observed the highest magnitude of elastic coefficient of 11 MPa (for the powder bed h = 100 mm) for sample 4. In contrary to this, the lowest magnitude of elastic

ACCEPTED MANUSCRIPT

coefficient of 0.95 MPa was observed for sample 2 for the same powder bed height. It was found in this study that the material stiffness characterised by the longitudinal elastic coefficient proportionally increased with increasing powder bulk density. The highest speed of sound (see eq. (1)) of the acoustic wave propagated through the powder bed (of 100 mm) was found for sample 1 (c = 121.6 m/s). This was attributed to the low sound absorption properties of sample 1 (hollow spheres) compared to the other materials tested. Most probably this phenomenon is caused by the observed closed cell porous structure of the individual hollow spheres. The mutual comparison of sound damping properties of the tested loose powder materials for the powder bed height h = 15 mm is shown in Fig. 3. It is evident that the best sound damping properties over the whole measured frequency range were obtained for sample 2. Contrary to this, the worst sound damping properties were found for the hollow sample 1, indicating its excellent sound reflecting properties. This result is in excellent agreement with the calculated values of the noise reduction coefficient NRC (Table 2), which represents the arithmetic mean sound absorption at the four given excitation frequencies. It was found that better sound absorption is obtained for materials with lower bulk density, hence exhibiting higher porosity. It was also evident (Figs. 2 and 3) that sound absorption is generally increasing with increasing excitation frequency [38].

The results of the powder bed aeration experiments are shown in Fig. 4 and Table 3. Basic flowability energy (BFE), aeration energy at 10 mm/s air velocity (AE_10), aeration ratio at 10 mm/s air velocity (AR_10) and normalised aeration sensitivity (NAS) parameters were determined. It was found that the spherical particle shape of sample 1 exhibited the lowest aeration energy of 7.5 mJ and the best fluidisation properties as reflected in the highest measured aeration ratio of 15.1 from all materials studied. These results are in excellent agreement with the most aerodynamic shape of the spherical particles in comparison to the plate like irregular particles which exhibit turbulent air flow patterns around the particles.

ACCEPTED MANUSCRIPT

Contrary to this, sample 2 was found to have low sensitivity to aeration across the whole range of air velocities tested. Such behaviour is typical for highly cohesive powder materials. The observed aeration energy for sample 2 was the highest in comparison to all materials studied at 25.1 mJ and the aeration ratio was the smallest of 3.6. Results of the aeration testing for samples 3 and 4 indicate that these powder materials are less cohesive and have moderate sensitivity to aeration. This fact indicates that samples 1, 3 and 4 create more compact powder bed structures compared with sample 2. This fact was confirmed in the sound absorption experiments, where sample 2 exhibited the best sound damping properties due to the more microporous structure of the powder bed (Table 2, Figure 3). This conclusion is also supported by the trend obtained for the basic flowability energy parameter, where the lowest magnitude was found for sample 2 at 90.8 mJ, whilst the BFEs for samples 1, 3 and 4 exceeded 107.9 mJ. The highest BFE was found for sample 4 at 179.3 mJ. The observed trends are in excellent agreement with the shear cell flow experiments. The hollow calcium carbonate spheres (sample 1) exhibited the highest flowability of 4.71, indicating easy flowing character [39], whereas samples 2, 3 and 4 showed cohesive properties (FF ranged between 3.01 (sample 3) to 3.81 (sample 4)).

It is well known from the literature, that the mechanical friction of individual nano/micro particles induces the creation of electrostatic charge on their surfaces [37]. This electrostatic charge has a strong influence on the packing density of the powder bed, thus influencing its mechanical, as well as acoustic properties. It was found in this study that the calcium carbonate hollow sphere particles (sample 1) were of positive electrostatic charge at 1.25 ± 0.22 nC, however lamellar precipitated calcium carbonate exhibited a negative electrostatic charge of -1.50 ± 0.24 nC. The highest charge was found for flash calcined kaolin (sample 2) at -10.15 ± 0.95 nC. Electrostatic charge of sample 3 (dolomite powder) was -4.17 ± 0.55 nC. The mutual comparison of the absolute values of the observed electrostatic charges of the

ACCEPTED MANUSCRIPT

samples studied was in the following order: sample 1<sample 4<sample 3<sample 2. This order was found to be of the same pattern as for the sound damping performance, where the best damping properties were found for sample 2 and the worst for sample 1. These results can be attributed to the spatial ordering of the individual micro particles, thus creating a specific porous structure as reflected in the observed packing densities in the case of each sample studied. However, the poor sound absorption performance of sample 1 indicates its superior sound reflection properties.

Conclusions

In this paper the material properties of four powder filler materials for polyolefin composite parts production for the automotive and aerospace industry were studied. It was found that the particle shape has a strong effect on the acoustic and mechanical properties of the powder bed as influenced by the varying packing density. Moreover the hollow calcium carbonate spheres exhibited the best aerodynamic performance when aerated and were completely fluidised. Simultaneously they exhibited the easy flowing behaviour as reflected in the observed flowability of 4.71. Contrary to this, the flat lamellar geometry of the calcined kaolin resulted in the worse fluidisation behaviour, as the aeration energy was 2.5× higher at 18 mJ compared to the spherical particles (AE_10 = 7.5 mJ). The flash calcined kaolin and dolomite powders exhibited cohesive powder behaviour as reflected in the observed flowability of 3.67 and 3.01, respectively.

There was found to be a clear correlation between powder rheological and electrostatic charge data, with the observed acoustic performance as reflected in the frequency dependency of the normal incident sound damping coefficient. Here a clear increase of the damping efficiency with increasing porosity of the powder bed was demonstrating as reflected in the decreasing packing density. However the best correlation with sound damping performance was found

ACCEPTED MANUSCRIPT

with the observed absolute values of the electrostatic charge of the tested powders. Here the largest electrostatic charge was found for sample 2 and the lowest for sample 1 (hollow spheres). The same pattern was also found for the sound damping performances, i.e. the best sound damping properties were found for sample 2 and the worst one for sample 1 (hollow spheres). However, the poor sound absorption performance of the sample 1 indicates its superior sound reflection properties make it potentially commercially attractive for sound insulation applications. The same dependency was also found for the aeration measurements results, where the most cohesive character was found for sample 2 and the best fluidisation properties found for the low density hollow spheres (sample 1). Based on the above results it can be concluded that the combination of the powder rheological and electrostatic charge measurements can be used to predict the sound damping properties of the powder filler materials.

Acknowledgements

Financial support from the grant no. LO1305 of the Ministry of Education, Youth and Sports of the Czech Republic is gratefully acknowledged. Author M.R. would like to express his gratitude for the financing of his research by AkzoNobel N.V. and the EPSRC (UK). Authors would like to express their gratitude for surface charge measurements to Mgr. B. Prudilová (Palacky University in Olomouc).

References

[1] Lapčík L,Jr., Jindrová P, Lapčíková B, Tamblyn R, Greenwood R, Rowson N. Effect of the talc filler content on the mechanical properties of polypropylene composites. J Appl Polym Sci 2008;110(5):2742-2747.

ACCEPTED MANUSCRIPT

[2] Lapčíková B, Lapčík L, Jr., Smolka P, Dlabaja R, Hui D. Application of radio frequency glow discharge plasma for enhancing adhesion bonds in polymer/polymer joints. J Appl Polym Sci 2006;102(2):1827-1833.

[3] Ottani S, Valenza A, Lamantia F. Shear characterization of CaCO3-filled linear low-density polyethylene. Rheologica Acta 1988;27(2):172-178.

[4] Zhu BL, Wang J, Zheng H, Ma J, Wu J, Wu R. Investigation of thermal conductivity and dielectric properties of LDPE-matrix composites filled with hybrid filler of hollow glass microspheres and nitride particles. Composites Part B-Engineering 2015;69:496-506.

[5] Huang R, Li P. Elastic behaviour and failure mechanism in epoxy syntactic foams: The effect of glass microballoon volume fractions. Composites Part B-Engineering 2015;78:401-408.

[6] Porfiri M, Gupta N. Effect of volume fraction and wall thickness on the elastic properties of hollow particle filled composites. Composites Part B-Engineering 2009;40(2):166-173.

[7] Wang X, Feng J, Bai Y, Zhang Q, Yin Y. Synthesis, properties, and applications of hollow micro-/nanostructures. Chemical reviews 2016:DOI: 10.1021/acs.chemrev.5b00731.

[8] Donath E, Sukhorukov G, Caruso F, Davis S, Mohwald H. Novel hollow polymer shells by colloid-templated assembly of polyelectrolytes. Angewandte Chemie-International Edition 1998;37(16):2202-2205.

[9] Nakashima T, Kimizuka N. Interfacial synthesis of hollow TiO2 microspheres in ionic liquids. J Am Chem Soc 2003;125(21):6386-6387.

ACCEPTED MANUSCRIPT

[10] Peng Q, Dong Y, Li Y. ZnSe semiconductor hollow microspheres. Angewandte Chemie-International Edition 2003;42(26):3027-3030.

[11] Ras RHA, Kemell M, de Wit J, Ritala M, ten Brinke G, Leskela M, Ikkala O. Hollow inorganic nanospheres and nanotubes with tunable wall thicknesses by atomic layer deposition on self-assembled polymeric templates. Adv Mater 2007;19(1):102-+.

[12] Tang Z, Akiyama Y, Itoga K, Kobayashi J, Yamato M, Okano T. Shear stress-dependent cell detachment from temperature-responsive cell culture surfaces in a microfluidic device. Biomaterials 2012;33(30):7405-7411.

[13] Velev O, Furusawa K, Nagayama K. Assembly of latex particles by using emulsion droplets as templates .1. Microstructured hollow spheres. Langmuir 1996;12(10):2374-2384.

[14] White RJ, Tauer K, Antonietti M, Titirici M. Functional hollow carbon nanospheres by latex templating. J Am Chem Soc 2010;132(49):17360-17363.

[15] Yang H, Zeng H. Preparation of hollow anatase TiO_2 nanospheres via Ostwald ripening. J Phys Chem B 2004;108(11):3492-3495.

[16] Ruszala M, Rowson N, Grover L, Choudhery R. Low carbon footprint TiO_2 substitutes in paint: A review. International Journal of Chemical Engineering and Applications 2015;6(5):331.

[17] Kowalski A, Vogel M. Blankenship RM. Polymeric pigment particles. US Patent 1984(4427836).

[18] Kowalski A, Vogel M. Core sheath polymer particles production useful as opacifying agent. US Patent 1984(4469825).

ACCEPTED MANUSCRIPT

[19] McDonald C, Devon M. Hollow latex particles: synthesis and applications. Adv Colloid Interface Sci 2002;99(3):181-213.

[20] Cayre OJ, Biggs S. Hollow microspheres with binary porous membranes from solid-stabilised emulsion templates. Journal of Materials Chemistry 2009;19(18):2724-2728.

[21] zu Putlitz B, Landfester K, Fischer H, Antonietti M. The generation of "armored latexes" and hollow inorganic shells made of clay sheets by templating cationic miniemulsions and latexes. Adv Mater 2001;13(7):500-+.

[22] Hadiko G, Han Y, Fuji M, Takahashi M. Synthesis of hollow calcium carbonate particles by the bubble templating method. Mater Lett 2005;59(19-20):2519-2522.

[23] Kim S, Ko JW, Park CB. Bio-inspired mineralization of CO2 gas to hollow CaCO3 microspheres and bone hydroxyapatite/polymer composites. Journal of Materials Chemistry 2011;21(30):11070-11073.

[24] Enomae T, Sasaki K, Kim B, Onabe F. Anisotropy of internal stress related to paper surface roughening. Tappi Advanced Coating Fundamentals Symposium 1999:133-145.

[25] Enomae T, Tsujino K. Application of spherical hollow calcium carbonate particles as filler and coating pigment. Appita J 2004;57(6):493-493.

[26] Fair G, Lange F. Effect of interparticle potential on forming solid, spherical agglomerates during drying. J Am Ceram Soc 2004;87(1):4-9.

[27] Kleinecke K. Influence of fillers on rheological behavior of high-molecular-weight polyethylene melts .1. Flow behavior in shear-flow and extensional flow. Rheologica Acta 1988;27(2):150-161.

ACCEPTED MANUSCRIPT

[28] Pannert W, Winkler R, Merkel M. On the acoustical properties of metallic hollow sphere structures (MHSS). Mater Lett 2009;63(13-14):1121-1124.

[29] Vašina M, Hughes DC, Horoshenkov KV, Lapčík L. The acoustical properties of consolidated expanded clay granulates. Appl Acoust 2006;67(8):787-796.

[30] Hong Z, Bo L, Huang Guangsu. Sound absorption behavior of multiporous hollow polymer micro-spheres. Mater Lett 2006;60(29-30):3451-3456.

[31] Janousch C, Winkler R, Wiegmann A, Pannert W, Merkel M, Oechsner A. Simulation and experimental validation of acoustic properties of hollow sphere structures. Materialwissenschaft Und Werkstofftechnik 2014;45(5):413-422.

[32] Lapčík L, Cetkovský V, Lapčíková B, Vašut S. Materials for noise and vibration attenuation. Chem Listy 2000;94(2):117-122.

[33] Lapčík L, Vašina M, Lapčíková B, Valenta T. Study of bread staling by means of vibro-acoustic, tensile and thermal analysis techniques. J Food Eng 2016;178:31-38.

[34] Okudaira Y, Kurihara Y, Ando H, Satoh M, Miyanami K. Sound-absorption measurements for evaluating dynamic physical-properties of a powder bed. Powder Technol 1993;77(1):39-48.

[35] International Organization for Standardization, ISO 10534-2. Acoustics-Determination of sound absorption coefficient and impedance in impedance tubes-Part 2: Transfer-function method. ISO 10534-2:1998 1998;ISO 10534-2.

ACCEPTED MANUSCRIPT

[36] Lapčík L, Vašina M, Lapčíková B, Otyepková E, Waters KE. Investigation of advanced mica powder nanocomposite filler materials: Surface energy analysis, powder rheology and sound absorption performance. Composites Part B-Engineering 2015;77:304-310.

[37] Lapčík L, Otyepka M, Otyepková E, Lapčíková B, Gabriel R, Gavenda A, Prudilová B. Surface heterogeneity: Information from inverse gas chromatography and application to model pharmaceutical substances. Curr Opin Colloid Interface Sci 2016;24(August):64-71.

[38] Le AT, Gacoin A, Li A, Mai TH, El Waki N. Influence of various starch/hemp mixtures on mechanical and acoustical behavior of starch-hemp composite materials. Composites Part B-Engineering 2015;75:201-211.

[39] Lapčík L, Lapčíková B, Krásný I, Kupská I, Greenwood RW, Waters KE. Effect of low temperature air plasma treatment on wetting and flow properties of kaolinite powders. Plasma Chem Plasma Process 2012;32(4):845-858.

ACCEPTED MANUSCRIPT

ACCEPTED MANUSCRIPT

Figure headings

Figure 1. SEM images of the studied composites filler materials, where sample 1 = hollow calcium carbonate spheres, sample 2 = flash calcined clay, sample 3 = dolomite and sample 4 = calcined kaolin.

Figure 2. Sound absorption coefficient frequency dependence for sample 1 (hollow particles) for different powder bed heights: black circle – 5 mm, red triangle down – 10 mm, green square – 20 mm, yellow diamond – 50 mm and blue triangle up – 100 mm. Arrow indicates primary absorption peak frequency (f_{p1}). Inset: SEM image of sample 1 hollow sphere structure.

Figure 3. Sound absorption coefficient frequency dependence of studied powder materials. Measured at the powder bed height of 15 mm.

Figure 4. Total energy against fluidised velocity for the four mineral samples.

Figure 5. Yield locus and the Mohr´s circles of the tested materials as obtained by shear cell experiments at applied 9 kPa consolidation stress.

ACCEPTED MANUSCRIPT

ACCEPTED MANUSCRIPT

Table headings

Table 1. Studied samples labelling and description.

Table 2. Results of the acoustic and mechanical testing for the studied powder composites filler materials.

Table 3. Results of the aeration test of the studied powder composite filler materials.

Table 4. Results from the shear cell flow experiments, measured at the consolidation stress of 9 kPa and the temperature of 24 °C.

ACCEPTED MANUSCRIPT

ACCEPTED MANUSCRIPT

Table 1. Studied samples labelling and description.

Sample	Geometry	Description	Moisture [w.%]
1	Hollow sphere	Calcium carbonate, narrow particle size distribution, 4 μm diameter, density 2.4 g/cm^3.	0.9
2	Agglomerate	Opacilite (Imerys), flash calcined kaolin, d_{50} = 1.6 μm, density 2.1 g/cm^3.	0.9
3	Lamellar	Microdol H600 (Omya, Switzerland), dolomite powder, d_{50} = 5.5 μm, density 2.9 g/cm^3.	0.3
4	Lamellar	Polestar 200P (Imerys), calcined kaolin, d_{50} = 2 μm diameter, density 2.7 g/cm^3.	0.1

ACCEPTED MANUSCRIPT

Table 2. Results of the acoustic and mechanical testing for the studied powder composites filler materials.

Sample	Quantity	Material height h [mm]					
		5	10	15	20	50	100
1	α_{max} [–]	0.345	0.512	0.508	0.478	0.506	0.446
	$f_{\alpha max}$ [Hz]	6368	6392	6384	5624	5688	5768
	NRC [–]	0.112	0.149	0.180	0.167	0.167	0.163
	f_{p1} [Hz]	1584	808	544	520	312	304
	K [MPa]	0.421	0.438	0.446	0.725	1.631	6.196
	c [m·s^{-1}]	31.7	32.3	32.6	41.6	62.4	121.6
2	α_{max} [–]	0.860	0.727	0.757	0.805	0.779	0.774
	$f_{\alpha max}$ [Hz]	4840	5920	6344	5600	6312	5936
	NRC [–]	0.188	0.316	0.359	0.434	0.500	0.338
	f_{p1} [Hz]	3992	2351	1264	768	244	152
	K [MPa]	1.6445	2.282	1.484	0.974	0.614	0.954
	c [m·s^{-1}]	79.8	94.0	75.8	61.4	48.8	60.8
3	α_{max} [–]	0.579	0.729	0.647	0.627	0.690	0.685
	$f_{\alpha max}$ [Hz]	5920	6384	5928	4864	6384	6392
	NRC [–]	0.132	0.258	0.228	0.279	0.254	0.220
	f_{p1} [Hz]	1472	1296	520	512	272	240
	K [MPa]	0.732	2.268	0.822	1.416	2.498	7.778
	c [m·s^{-1}]	29.4	51.8	31.2	41.0	54.4	96.0
4	α_{max} [–]	0.571	0.563	0.639	0.635	0.580	0.644
	$f_{\alpha max}$ [Hz]	5760	6392	6376	6384	4864	5592
	NRC [–]	0.128	0.181	0.221	0.201	0.221	0.236
	f_{p1} [Hz]	1536	696	472	416	288	272
	K [MPa]	0.878	0.721	0.746	1.030	3.086	11.008
	c [m·s^{-1}]	30.7	27.8	28.3	33.3	57.6	108.8

ACCEPTED MANUSCRIPT

ACCEPTED MANUSCRIPT

Table 3. Results of the aeration test of the studied powder composite filler materials.

Sample	BFE [mJ]	AE_10 [mJ]	AR_10 [-]	NAS [s/mm]
1	114.1	7.5	15.1	0.344
2	90.8	25.1	3.6	0.152
3	107.9	13.4	8.1	0.261
4	179.3	18.0	9.9	0.310

ACCEPTED MANUSCRIPT

ACCEPTED MANUSCRIPT

Table 4. Results from the shear cell flow experiments, measured at the consolidation stress of 9 kPa and the temperature of 24 °C.

Sample	Cohesion [kPa]	UYS [kPa]	MPS [kPa]	FF [-]	AIF [°]	BD [g/ml]	MCS [kPa]	AIF [E] [°]
1	0.86	2.98	14.04	4.71	30.13	1.95	3.67	35.86
2	1.30	4.74	17.38	3.67	32.55	1.17	3.80	39.89
3	1.48	5.72	17.23	3.01	35.34	1.92	3.07	44.20
4	1.15	4.36	16.62	3.81	34.53	2.36	3.39	41.39

UYS – unconfined yield strength, MPS – major principal stress, FF – flow function, AIF – angle of internal friction, DB – bulk density, MCS – minor consolidation stress, AIF [E] – angle of internal friction (effective).

ACCEPTED MANUSCRIPT

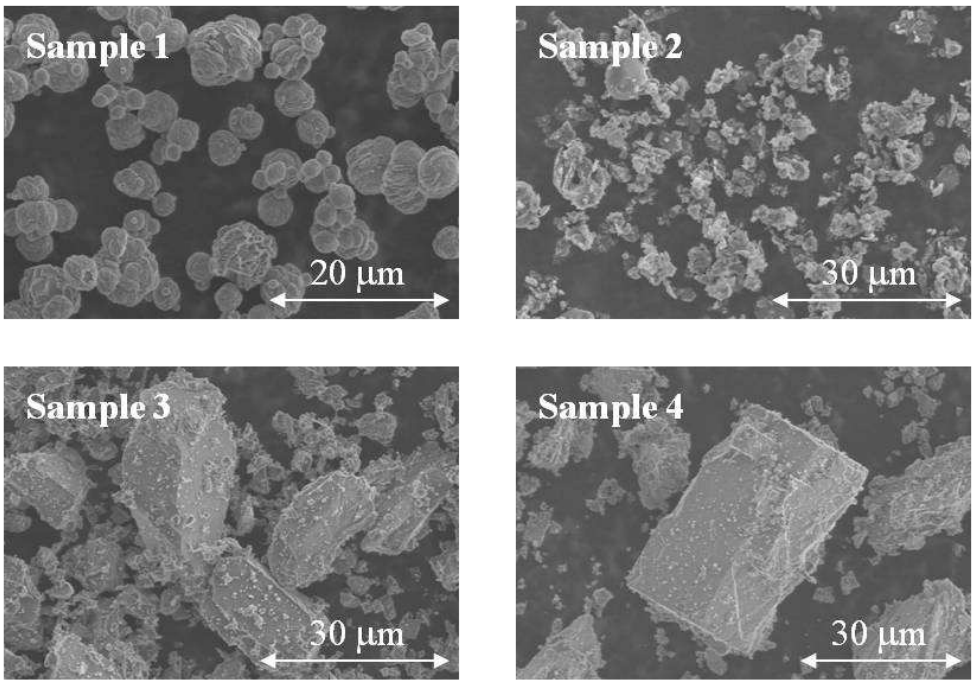

Figure 1. SEM images of the studied composites filler materials, where sample 1 = hollow calcium carbonate spheres, sample 2 = flash calcined clay, sample 3 = dolomite and sample 4 = calcined kaolin.

ACCEPTED MANUSCRIPT

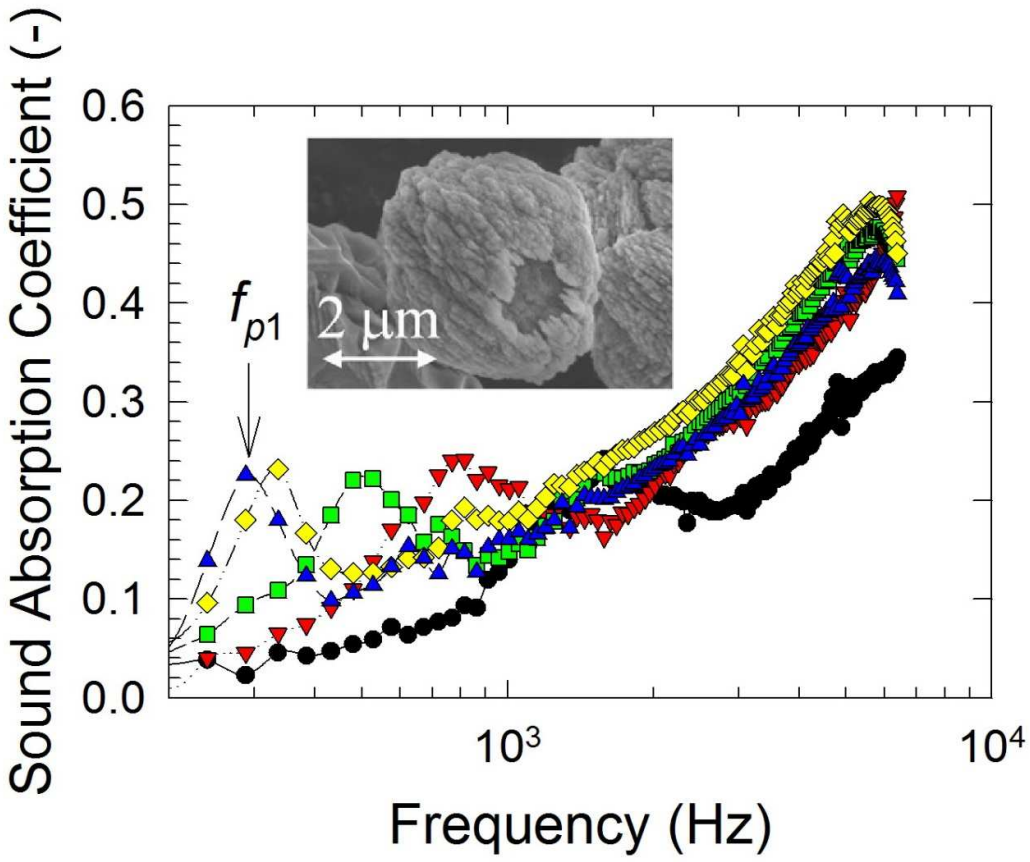

Figure 2. Sound absorption coefficient frequency dependence for sample 1 (hollow particles) for different powder bed heights: black circle – 5 mm, red triangle down – 10 mm, green square – 20 mm, yellow diamond – 50 mm and blue triangle up – 100 mm. Arrow indicates primary absorption peak frequency (f_{p1}). Inset: SEM image of sample 1 hollow sphere structure.

ACCEPTED

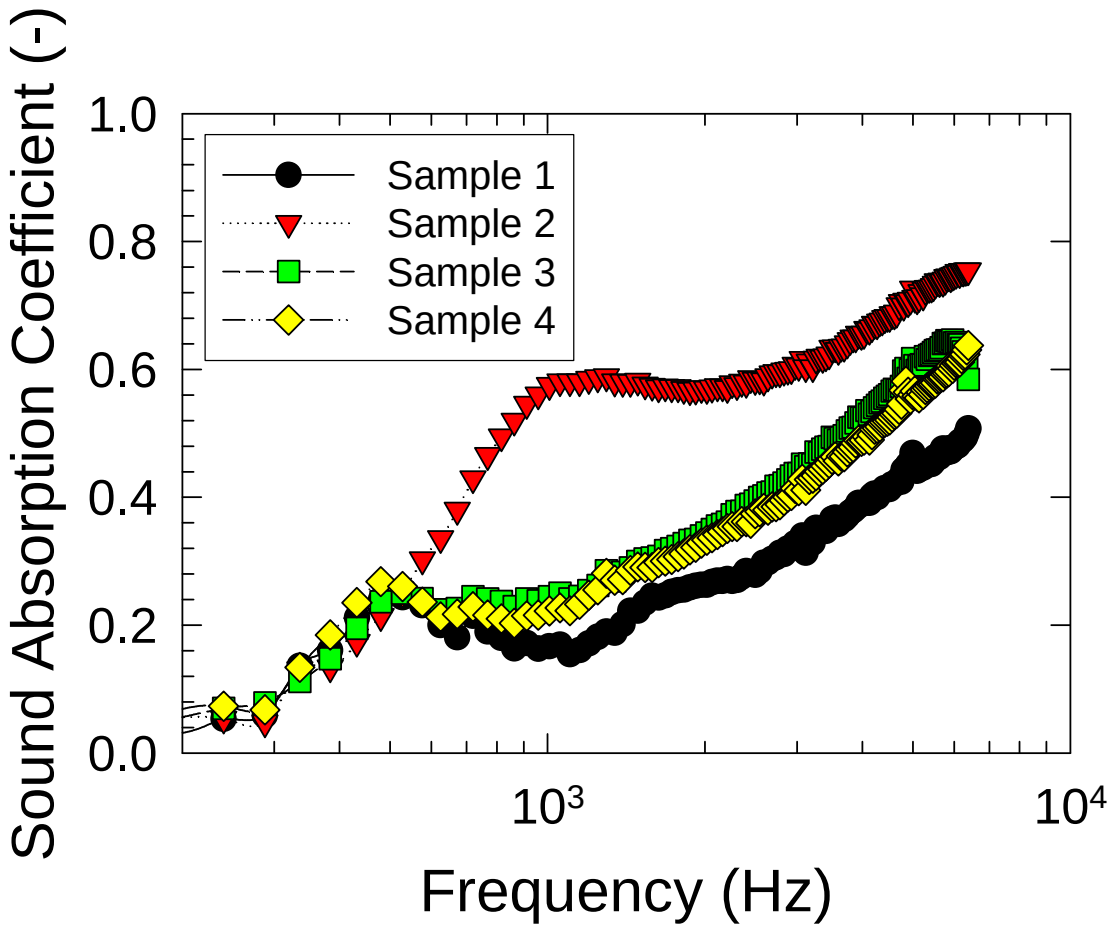

Figure 3. Sound absorption coefficient frequency dependence of studied powder materials.

Measured at the powder bed height of 15 mm.

ACCEPTED

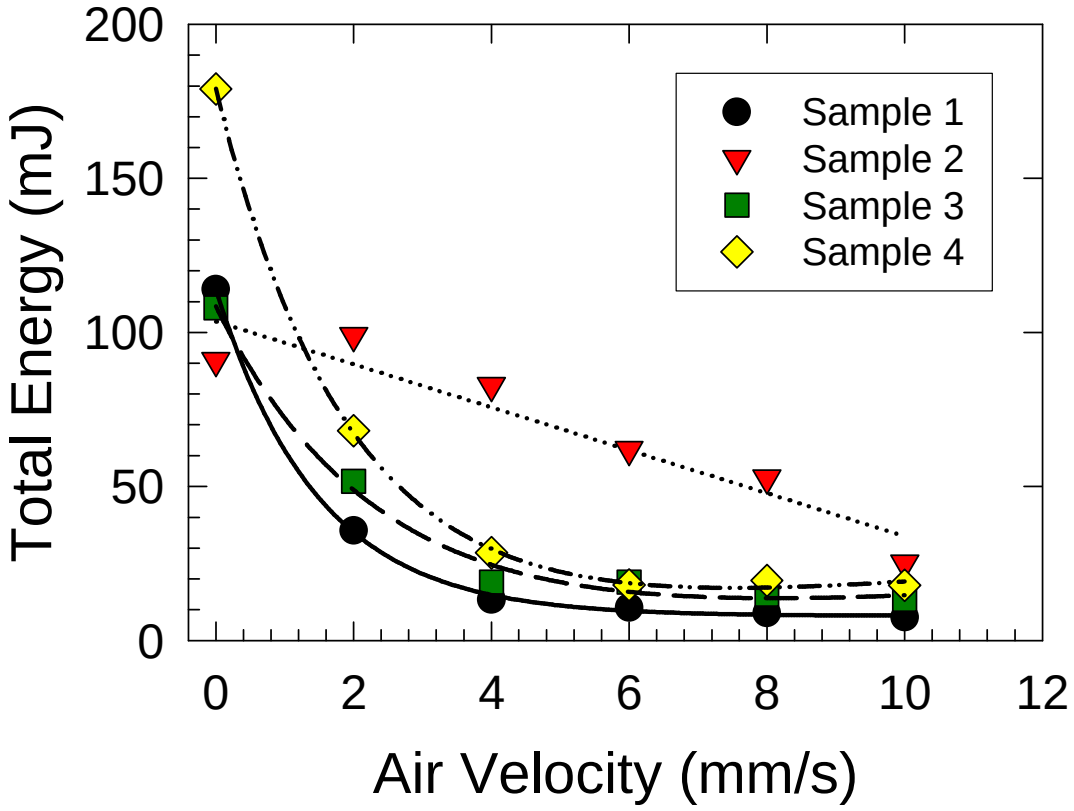

Figure 4. Total energy against fluidised velocity for the four mineral samples.

ACCEPTED MANUSCRIPT

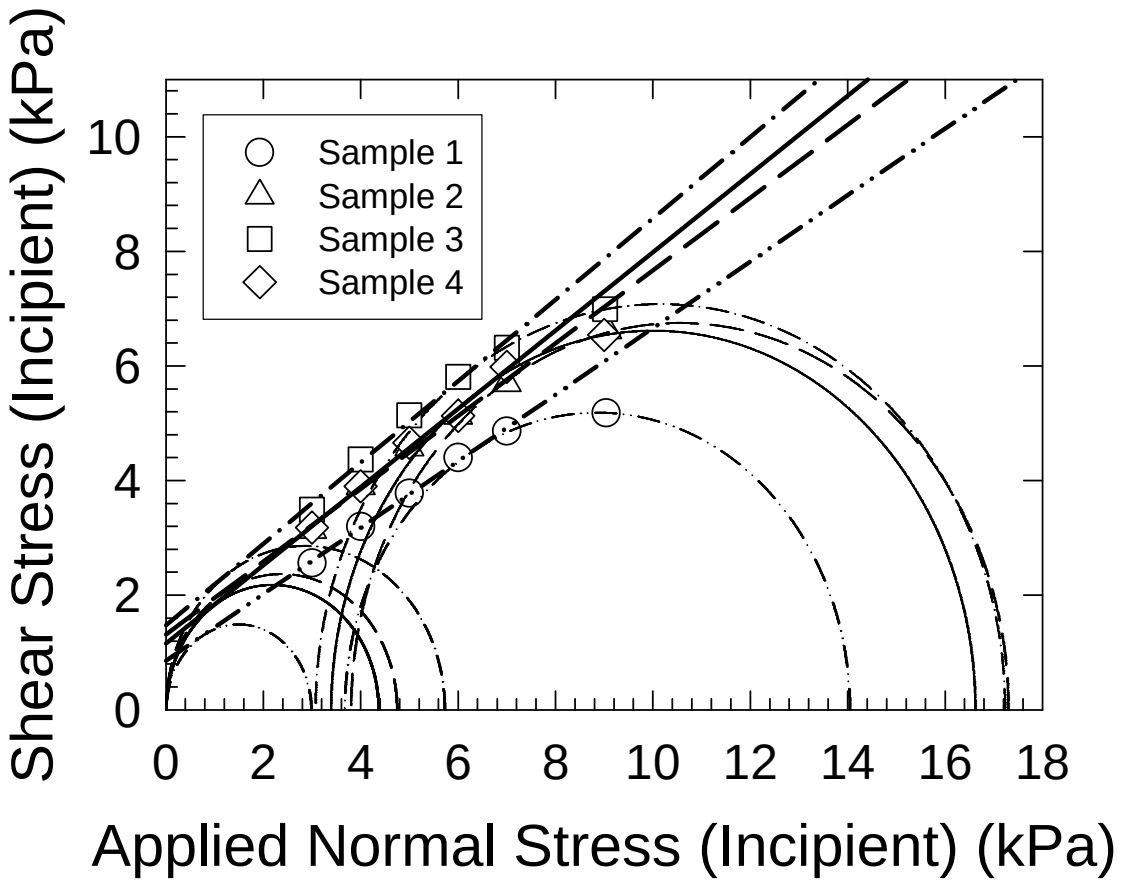

Figure 5. Yield locus and the Mohr´s circles of the tested materials as obtained by shear cell experiments at applied 9 kPa consolidation stress.

ACCEPTED MANUSCRIPT

ACCEPTED MANUSCRIPT

Highlights

Four types of powder filler materials for composite parts production were studied.

Particle shape has a strong effect on the acoustic and mechanical properties of the powders.

A clear correlation between electrostatic charge and acoustic performance was found.

Hollow spheres demonstrated superior sound reflection properties.

ACCEPTED MANUSCRIPT